Differentiating mechanism from outcome for ancestry-assortative mating in admixed human populations

Dashiell J. Massey[1], Zachary A. Szpiech[2,3], Amy Goldberg[1,4]

[1] Department of Evolutionary Anthropology, Duke University, USA 27708

[2] Department of Biology, Pennsylvania State University, USA 16802

[3] Institute for Computational and Data Sciences, Pennsylvania State University, USA 16802

[4] Corresponding author: amy.goldberg@duke.edu

Abstract

Population genetic theory, and the empirical methods built upon it, often assume that individuals pair randomly for reproduction. However, natural populations frequently violate this assumption, which may potentially confound genome-wide association studies, selection scans, and demographic inference. Within several recently admixed human populations, empirical genetic studies have reported a correlation in global ancestry proportion between spouses, referred to as ancestry-assortative mating. Here, we use forward genomic simulations to link correlations in global ancestry proportion between mates to the underlying mechanistic mate-choice process. We consider the impacts of two types of mate-choice model, using either ancestry-based preferences or social groups as the basis for mate pairing. We find that multiple mate-choice models can produce the same correlations in global ancestry proportion between spouses; however, we also highlight alternative analytic approaches and circumstances in which these models may be distinguished. With this work, we seek to highlight potential pitfalls when interpreting correlations in empirical data as evidence for a particular model of human mating practices, as well as to offer suggestions toward development of new best practices for analysis of human ancestry-assortative mating.

Introduction

Non-random mating has long been appreciated as an important source of genetic structure in natural populations (Fisher 1918; Wright 1921; Wright 1950; Nagylaki 1978). Positive assortative mating (hereafter, assortative mating), wherein genotypic or phenotypic trait values are positively correlated between mates, has been empirically observed across animal species (Jiang *et al.* 2013). Theoretical and empirical studies have demonstrated the consequences of assortative mating for speciation and hybridization (Kondrashov 1983; Otto *et al.* 2008; Tung *et al.* 2012; Schumer *et al.* 2017; Kopp *et al.* 2018; Powell *et al.* 2021; Muralidhar *et al.* 2022; Natola *et al.* 2022; Smadja *et al.* 2022; Robinson *et al.* 2023), and for the distributions of traits within populations (Wright 1921; Norris *et al.* 2019; Kim *et al.* 2021; Border *et al.* 2022; Muralidhar *et al.* 2022; Horwitz *et al.* 2023).

In non-human primates that live in complex and structured social environments, sociodemographic factors have also been demonstrated to influence mate pair formation (Keddy-Hector 1992; Klinkova *et al.* 2005; Setchell and Wickings 2006; Van Belle *et al.* 2009; Tung *et al.* 2012; Fogel *et al.* 2021). As such, when it comes to humans, assortative mating has been the purview not only of biologists, but also social scientists (*e.g.*, (Buss and Barnes 1986; Mare 1991; Kalmijn 1998; Luo and Klohnen 2005; Blossfeld 2009; Torche 2010; Schwartz 2013; Greenwood *et al.* 2014; Henz and Mills 2017; Smieja and Stolarski 2018; Chiappori 2020; De La Mare and Lee 2023)). Positive correlations have been reported between human spouses for a diverse array of phenotypes, including morphometric measurements, health outcomes, personality traits, lifestyle factors, age, socioeconomic status, educational attainment, religious affiliation, and language (Nagoshi *et al.* 1990; Robinson *et al.* 2017; Fibla *et al.* 2022; Horwitz *et al.* 2023; Yamamoto *et al.* 2023). These associations are likely driven by multiple generative processes, including individual mate-choice preferences, phenotypic convergence over time facilitated by cohabitation, and social structures that restrict or promote particular pairings. These processes may act individually or in concert. For instance, sociological literature on assortative mating by educational attainment has revealed the influence of both a preference for mate similarity (Kalmijn 1998) and social barriers to marriage across socioeconomic class (Torche 2010), and that the strength of assortment by education over time is sensitive to the degree of temporal overlap between the end of schooling and average age at the time of marriage (Mare 1991), suggesting that social milieu is likely also an important factor in structuring mate pair outcomes.

Within the field of population genetics, relatively less attention has been paid to understanding the contributions of these generative processes to producing the observed correlations between mating pairs. Indeed, mechanism and outcome are often conflated or not clearly delineated when discussing assortative mating, which obscures these multiple mechanisms that may contribute to mate similarity. When studies do consider mechanism, they typically draw on foundational work in the sexual selection literature modeling the effects of female choice on male phenotype (Lande 1981; Kirkpatrick 1982; Seger 1985), in which the mechanism driving assortative mating is assumed to be mate choice. To extend this framework beyond sexual dimorphism, the mate-choice mechanism is modeled as a preference for mates that "match" an individual's own phenotype (Kopp *et al.* 2018; Goldberg *et al.* 2020; Kim *et al.* 2021; Muralidhar *et al.* 2022). However, some studies have suggested that temporal structure in the mating process (Xie *et al.* 2015; Woodman *et al.* 2023) or non-uniform ability to attract mates (Burley 1983) can generate phenotypic correlations between mates without an explicit preference for phenotypic similarity. In this paper, we use the term

"assortative mating" to refer specifically to an empirical observation of greater resemblance between mates than expected by chance, agnostic to mechanism.

Reports of assortative mating by ancestry in humans provide a particularly intriguing example for exploring mechanism because genetic ancestry is a complex quantitative "phenotype" that involves every locus in the genome and that can only be ascertained by sequencing. In recently admixed human populations, in which individuals derive ancestry from multiple source populations, a positive correlation in global ancestry proportion between spouses has been observed. This phenomenon, referred to as ancestry-assortative mating, has been reported in multiple Latino populations (Risch *et al.* 2009; Zou *et al.* 2015; Spear *et al.* 2020; Mas Sandoval *et al.* 2023), as well as in African-Americans (Zaitlen *et al.* 2017; Avadhanam and Williams 2022), Cabo Verdeans (Korunes *et al.* 2022), and ni-Vanuatu (Arauna *et al.* 2022). Ancestry-associated mating patterns, inferred from excess sharing of single-nucleotide variants, have also been reported for non-Hispanic white spouse pairs in the United States (Sebro *et al.* 2010; Domingue *et al.* 2014; Sebro *et al.* 2017). Empirical studies commonly use such correlations in global ancestry proportion between spouses to suggest that ancestry shapes mate choice, although this interaction would necessarily be mediated by a proxy phenotype of some type, not by quantitative ancestry proportion. However, the relative contributions of individual preferences and broader social mechanisms to generating these correlations are unclear.

Accounting for assortative mating is critical for accurate statistical and population genetic analysis in admixed human populations: it has been shown that assortative mating confounds genome-wide association studies (Howe *et al.* 2021; Border *et al.* 2022; Veller and Coop 2024) and heritability estimation (Sebro and Risch 2012; Tenesa *et al.* 2016; Huang *et al.* 2024). In addition, ancestry-assortative mating specifically has been shown to produce estimates for the timing of admixture that are too recent (Zaitlen *et al.* 2017; Goldberg *et al.* 2020; Korunes *et al.* 2022). However, it remains challenging to establish a null expectation in the presence of assortative mating without understanding the underlying mechanism at play.

To date, statistical methods to correct for ancestry-assortative mating in empirical data have tended to generate null models by simulating data to match the observed empirical correlation in global ancestry proportion between mating pairs, often without a specific mechanistic model (Zaitlen *et al.* 2017; Spear *et al.* 2020; Pfennig and Lachance 2023; Huang *et al.* 2024). This approach makes two important assumptions: first, that the correlation coefficient for a given population has remained constant over time; and second, that matching the correlation coefficient is sufficient to recapitulate the dynamics of global and local ancestry. In contrast, theoretical population genetic studies have examined the behavior of these same parameters using mechanistic models of biased mate choice (Goldberg *et al.* 2020; Kim *et al.* 2021; Muralidhar *et al.* 2022). This approach assumes that ancestry-based preference is the primary mechanism driving non-random mating. These studies typically do not directly consider whether the model used results in an observed correlation in global ancestry proportion between mates, which leaves open the question of how applicable their conclusions are to the context of empirical studies of human ancestry-assortative mating.

Here, we used forward-in-time simulations to probe the relationship between mate-choice mechanism and observed correlation in global ancestry proportion, comparing variants of two classes of mate-choice model. The first model class considers only individual mate-choice

preferences for similarity in global ancestry proportion, treating genetic ancestry as a continuous quantitative trait. The second class considers only discrete social groups, assigning each individual to one of two groups and limiting cross-group mating events. (Importantly, group membership is "inherited" from one parent and group identities are initially associated with source populations; see **Models**.) We found that ancestry-similarity and social group models can produce similar correlations in global ancestry proportion between mates, suggesting that either or both mechanisms could be relevant in interpreting empirical data. Furthermore, the correlation coefficient was not constant over time in any of our simulations, and not all variants of the ancestry-similarity class or all parameter values of the social-group model maintained sufficient population variance to sustain correlations in global ancestry proportion over tens of generations. Our results highlight important caveats about the assumptions behind both existing approaches and suggest additional analyses of empirical data that may help reveal the underlying mechanism of ancestry-assortative mating in human populations.

Models

Simulation framework

We performed forward-in-time simulations of admixture with equal contributions from two source populations using SLiM 4.0.1 (HALLER *et al.* 2019; HALLER AND MESSER 2023). We modeled sexually reproducing diploid individuals (census population size $N = 10{,}000$/generation) with 22 independently segregating chromosomes, representing the size distribution of human autosomes (total genome size $L = 2.88$ Gb), with a uniform recombination rate $r = 1 \times 10^{-8}$. Unless otherwise noted, there was a single pulse of admixture and no additional contributions from the source populations introduced at later generations. We did not model any type of one- or two-dimensional spatial relationships between individuals, nor did we simulate genotypes.

For each of 50 generations post-admixture, we extracted the position and source of local-ancestry tracts from the tree-sequence (HALLER *et al.* 2019). From these data, we calculated the total proportion of the genome that each individual derived from source population 1 (hereafter, global ancestry proportion, $x \in [0,1]$). Separately, we tracked the social group $s \in \{A, B\}$ to which each individual belonged: offspring were assigned to the same social group as their first parent – *i.e.*, without reference to their global ancestry proportion. We focus primarily on results from the first 20 generations post-admixture, approximately corresponding to the timing of African-European admixture initiated by the trans-Atlantic slave trade (ZAITLEN *et al.* 2017; HAMID *et al.* 2021; KORUNES *et al.* 2022; MAS SANDOVAL *et al.* 2023; MOONEY *et al.* 2023), with a subset of results over longer time periods in the Supplement.

We considered two broad classes of mate-choice models: (1) **ancestry-similarity**, wherein the probability of an individual with global ancestry proportion x_i mating with an individual with global ancestry proportion x_j is defined in terms of $|x_i - x_j|$; and (2) **social group**, wherein the probability of an individual belonging to social group s_i mating with an individual belonging to social group s_j is defined by whether or not $s_i = s_j$.

To implement non-random mating in SLiM, we started from the default Wright-Fisher framework, which is designed to allow females to be selective if a `mateChoice()` callback is used. In this work, we did not distinguish males and females, instead allowing each individual to potentially serve as both parent 1 (selector) and parent 2 (selected) in sequential mating events. For each mating event, parent 1 was uniformly sampled with replacement from the population, while parent 2 was sampled proportional to mating weight $\psi_{i,j}$, calculated according to the specified mate-choice function (defined below) evaluated for $f(x_i, x_j)$ or $f(s_i, s_j)$, under the ancestry-similarity and social group models, respectively (**Figure 1**). Incidental selfing was explicitly prohibited and each mating event generated a single child.

Defining a common parameter for model comparison

The mate-choice functions we considered (EQUATIONS 3-6, below) differ in how they parameterize the strength of mating bias; to aid in comparison across models, we will refer throughout to $\alpha \in [0, \infty)$, the frequency of mating events between individuals from opposite source populations.

Specifically, we define α to be inversely related to the proportion of admixed offspring in the initial generation post-contact, A. We have,

$$\alpha = \frac{1}{\mathrm{A}} - 1. \tag{1}$$

That is, at time of population contact, individuals are α times more likely choose a mate from within their own source population than from the opposite source population. Increasing values of α representing an increasing bias toward endogamy, with $\alpha = 0$ corresponding to exclusive exogamy, $\alpha \in (0,1)$ to negative assortative mating, $\alpha = 1$ to random mating, and $\alpha > 1$ to positive assortative mating. Given our focus on mechanisms that might explain empirically observed positive correlations in global ancestry proportion between mates, we consider only $\alpha \geq 1$. While our models differ in their dynamics over time, simulations with the same α have the same correlation in global ancestry proportion between mates, $r(x_i, x_j) \in [0,1]$, for the first generation post-admixture under all models.

Ancestry-similarity models

Individual-based mate preference models originate in the sexual selection literature, where they were developed for studying the co-evolutionary dynamics of male secondary sex characteristics and female mate choice (LANDE 1981; KIRKPATRICK 1982; SEGER 1985). Generally, under these models, male phenotype and female preference are controlled by distinct genetic loci (or sets of loci). In the speciation literature, an alternative family of models are concerned with assortative mating as a mechanism of sympatric speciation and model mate preference based on phenotypic similarity between mates for some ecologically relevant trait (DIECKMANN AND DOEBELI 1999; BURGER AND SCHNEIDER 2006; PENNINGS *et al.* 2008; RETTELBACH *et al.* 2013). These "matching rule" models (KOPP *et al.* 2018) are the basis for our ancestry-similarity model class, wherein individuals preferentially choose mates to maximize similarity in phenotype (*i.e.*, global ancestry proportion). Importantly for the models we consider here, these are fixed relative-preference models: a focal individual i assigns each potential mate a preference value $\psi_{i,j}$ that depends only on the potential mate's phenotype and is density independent (SEGER 1985).

Ancestry-similarity models define a mate-choice function $\psi_{i,j} = f(x_i, x_j)$ for calculating the sampling weight assigned to individual j with global ancestry proportion x_j as a potential mate for a focal individual i with global ancestry proportion x_i. In the present study, we considered three variants of the ancestry-similarity model identified in a literature search, which differ in the precise definition of the mate-choice function f.

Models of ancestry-based assortative mating typically model $f(x_1, x_i)$ as an exponential function, such that $\psi_{i,j}$ decays exponentially at rate $c = \ln(\alpha)$ as $|x_i - x_j|$ increases. We define,

$$\psi_{i,j} = e^{-c|x_i - x_j|}. \tag{2}$$

We refer to this as the **stationary-preference model** ("like-with-like" model in (MURALIDHAR *et al.* 2022)): for a given absolute difference in global ancestry proportion, $|x_i - x_j|$, the associated preference $\psi_{i,j}$ does not change over time. It is important to note, however, that the range of $\psi_{i,j}$ is

constrained by x_i: an individual i with global ancestry proportion $x_i = 0.5$ is more similar to all potential mates than an individual with $x_i = 0$, and is therefore less selective in choosing a mate (**Figure 1a**). Furthermore, without additional migration from the source populations, variance in global ancestry proportion across individuals decreases over time (**Figure S2**), meaning that the pool of potential mates is becoming increasingly homogenous and the ratio of $\max(\psi_{i,j})/\min(\psi_{i,j})$ approaches 1 for all values of x_i (**Figure S1a**). In other words, all individuals become less selective in choosing mates over successive generations.

One approach to account for the decreased variance in global ancestry proportion over time, and thus preserve mate-selectiveness, is to decrease c, rather that holding it constant. Following (KIM *et al.* 2021), we re-scale c in each generation t using the variance in global ancestry proportion observed in that generation, $\sigma_x^2(t)$:

$$\psi_{i,j} = e^{\frac{-c}{\sigma_x^2(t)}|x_i - x_j|}. \quad (3)$$

We refer to this as the **increasing-preference model** (EQUATION A2 in (KIM *et al.* 2021)). Under this model, as under the stationary-preference model, an individual i with global ancestry proportion $x_i = 0.5$ is less selective than one with $x_i = 0$ (**Figure 1b**). However, because $\sigma_x^2(t)$ decreases over time, there is an increase in mate-selectiveness over successive generations under this model for a given x_i (**Figure S1b; Figure S3**).

We also considered a third ancestry-similarity model, employing a Gaussian – rather than exponential – mate-choice function. This approach is commonly used in models of assortative mating based on a quantitative trait (*e.g.,* (DIECKMANN AND DOEBELI 1999; PENNINGS *et al.* 2008; FUNK *et al.* 2021)), although it has not to our knowledge been used to model assortative mating based on global ancestry proportion. Under this model, $\psi_{i,j} \sim N(x_i, \sigma^2)$ where x_i is the global ancestry proportion of the focal individual and the constant $\sigma^2 = \frac{1}{\sqrt{-2\ln(\alpha^{-1})}}$ determines the strength of mate-choice preference. Again, $\psi_{i,j}$ decreases as the difference in global ancestry proportion between potential mates increases:

$$\psi_{i,j} = \frac{1}{\sigma\sqrt{2\pi}} e^{-\frac{(x_i - x_j)^2}{2\sigma^2}}. \quad (4)$$

We refer to this as the **broad-preference model** because $f(x_i, x_j)$ decays more gradually with increasing differences in global ancestry proportion, relative to the stationary-preference and increasing-preference models (**Figure 1c**). Thus, a large difference in global ancestry proportion from a potential mate is strongly disfavored, while smaller differences within the pool of "similar" mates are not weighed strongly. Compared to the other two ancestry-similarity models, individuals are less selective in choosing mates under the broad-preference model; however, as under the stationary-preference model, they also become less selective over time (**Figure S1c; Figure S4**).

Social group model

An alternative class of models considers preferential mating based on a categorical, rather than quantitative, trait. This type of model is often used in the context of interspecific hybrid zones,

wherein non-random mating can maintain species boundaries and/or promote hybrid speciation (MELO *et al.* 2009; SCHUMER *et al.* 2017; POWELL *et al.* 2021; NATOLA *et al.* 2022; SMADJA *et al.* 2022). Mechanistically, this can be construed as a model of biased mating by species identity or source population (GOLDBERG *et al.* 2020). However, application of this type of model in humans is not straightforward: the source populations in question are not biologically distinct species, but rather labels describing socially and geographically defined boundaries that have changed over time. Furthermore, it is unclear how we ought to model the mating behavior of admixed individuals: neither random mating by admixed individuals nor a simple preference of admixed individuals to mate with one another seem likely to produce the observed correlation in global ancestry proportion between mates. Yet, the strongest evidence for ancestry-assortative mating in humans is observed in contexts where both spouses have admixed ancestry (RISCH *et al.* 2009; ZOU *et al.* 2015; ZAITLEN *et al.* 2017; SPEAR *et al.* 2020; AVADHANAM AND WILLIAMS 2022; KORUNES *et al.* 2022; MAS SANDOVAL *et al.* 2023).

Social identity is an important organizer of pair formation in humans, as evidenced by widespread cultural practices of endogamy based on race, ethnicity, religion, socioeconomic status, and caste. Although distinct from genetic ancestry, social categorizations often interact with ancestry. For instance, skin pigmentation, a prominent contributor to how an individual is racialized, is correlated with West African-related global ancestry proportion in multiple populations with recent admixture history (PARRA *et al.* 2003; SHRIVER *et al.* 2003; BONILLA *et al.* 2004; BELEZA *et al.* 2012). Race has also served as the basis for numerous sociolegal barriers to mating across contexts, including anti-miscegenation laws (BROWNING 1951). This type of interaction opens the possibility that social barriers to mating might be "recorded" in patterns of ancestry-assortative mating detectable by genomic analyses.

We considered a simple **social group model** with two groups, with sampling weight $\psi_{i,j}$ determined by the social group identity of the focal individual and potential mate, s_i and s_j, respectively, with preference strength α (**Figure 1d; Figure S5**). Rearranging EQUATION 1:

$$\psi_{i,j} = \begin{cases} 1 - \dfrac{1}{\alpha + 1}, & s_i = s_j \\ \dfrac{1}{\alpha + 1}, & s_i \neq s_j. \end{cases} \quad (5)$$

To generate an association between social group membership and global ancestry proportion, we assigned individuals in each source population to the same social group prior to admixture. However, from the onset of population contact, individuals "inherited" their social group membership from the first parent in the mating pair. Thus, individuals whose parents belonged to opposite social groups were equally likely to be assigned to either social group.

Several features distinguish the social group model from the ancestry-similarity models described above, or from one in which individuals use an observable quantitative trait (*e.g.*, skin pigmentation) as a proxy for an unobserved trait (global ancestry proportion). First, social group membership is correlated with – but not determined by – genotype. This matters because it has previously been demonstrated that recombination is expected to decouple the relationship between global ancestry proportion and a proxy quantitative trait over time, leading to only a transient correlation between the two phenotypes (KIM *et al.* 2021). Because social group

membership is not genetic, it is not impacted by recombination. In addition, individuals are uniformly likely to cross the social group barrier in choosing a mate and do not express relative preferences among potential mates within a social group. Thus, in contrast to an ancestry-similarity model, individuals with intermediate ancestry are not less selective than individuals with more source-like ancestry in choosing a mate.

However, these features of the social group model also mean that the association between global ancestry proportion and social group membership is expected to decay over successive generations, and we explored this relationship quantitatively over time.

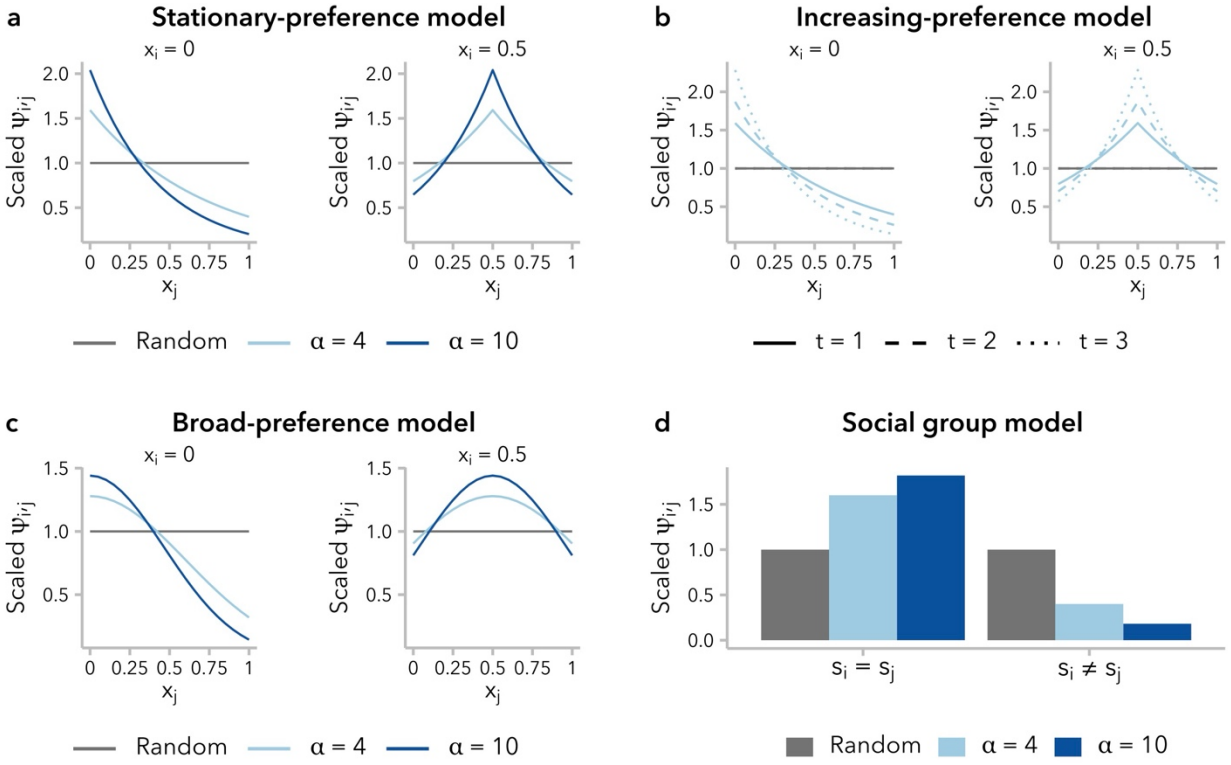

Figure 1. Four functions for defining the sampling weight, $\psi_{i,j}$, assigned to individual j as a potential mate for a focal individual i, based on global ancestry proportion x_j (**a-c**) or social group s_j (**d**). For each mating event, mate 1 was uniformly sampled from the population, and mate 2 was sampled proportional to $\psi_{i,j}$. For the sake of visualization, values of $\psi_{i,j}$ have been scaled such that $\psi_{i,j} = 1$ means that the probability of individual j being selected as a potential mate for individual i is $1/n$ (n: number of potential mates). All mate-choice functions are re-parameterized in terms of α. **(a)** The stationary-preference variant of the ancestry-similarity model (EQUATION 2) defines $\psi_{i,j}$ as a function of the difference in global ancestry proportion between individuals, $|x_i - x_j|$. **(b)** Under the increasing-preference variant of the mate-preference model (EQUATION 3), the value of $\psi_{i,j}$ is scaled to the variance in global ancestry proportion, $\sigma_x^2(t)$, across all potential mates, resulting in increasing choosiness over time. $\psi_{i,j}$ values are shown for $t \in \{1,2,3\}$ and $\alpha = 4$, assuming $\sigma_x^2(t) = 2^{-\frac{t}{2}}$ (LIANG *et al.* 2024). **(c)** Under the broad-preference variant of the ancestry-similarity model (EQUATION 4), $\psi_{i,j}$ follows the probability density function of a normal distribution with mean x_i. **(d)** Under the social group model (EQUATION 6), $\psi_{i,j}$ can take one of two discrete values, determined by whether a potential mate belongs to the same social group as the focal individual ($s_i = s_j$) or to the other social group ($s_i \neq s_j$).

Results

Not all simulations of non-random mating show a positive correlation in global ancestry proportion between mates 20 generations post-admixture

Ancestry-assortative mating is often inferred from a positive correlation in global ancestry proportion between spouses at single point in time, and statistical methods to account for non-random mating typically generate null models using simulations where potential mate pairs are permuted until the empirically observed correlation is achieved (ZAITLEN *et al.* 2017; PFENNIG AND LACHANCE 2023; HUANG *et al.* 2024). This approach assumes that the correlation observed in the present-day samples has remained constant since the start of admixture. **Figure 2** plots the Pearson correlation coefficient for global ancestry proportion between mates, $r(x_i, x_j)$, over time under three variants of the ancestry-similarity model or the social group model, for multiple strengths of mating bias, α, and following a single pulse of admixture. In all scenarios of non-random mating that we considered, we observed positive correlations in global ancestry proportion between mates (**Figure 2; Figure S6**). However, contrary to the assumption that the correlation observed in a contemporary sample should be modeled as a fixed value, the observed correlation coefficients in our simulations decayed over time. In simulations performed under the increasing-preference model, $r(x_i, x_j)$ reached a stable plateau within the first 10 generations post-admixture across values of α (**Figure S7a**). In contrast, simulations performed under the other two variants of the ancestry-similarity model (stationary-preference or broad-preference) approached $r(x_i, x_j) = 0$ within 20 generations post-admixture, unless α was sufficiently large to disrupt the admixture process altogether (**Figure S8; Figure S9**). Under the social group model, positive values of $r(x_i, x_j)$ could be observed 20 generations post-admixture for $\alpha > 2$, although these models also approached $r(x_i, x_j) = 0$ on longer time scales (**Figure S7b**).

To formally test whether the decay in $r(x_i, x_j)$ meant that mating was effectively random at $t = 20$ generations post-admixture under the stationary-preference and broad-preference models, we permuted the mating pairs and re-calculated $r(x_i, x_j)$ for 1,000 permutations of the simulated data. For the stationary-preference model, we found examples in which $r(x_i, x_j)$ was close to – but still significantly different from – zero by a permutation test. For instance, for the five replicate simulations with $\alpha = 10$, $r(x_i, x_j) \in [0.0182, 0.0444]$ for $t = 20$ generations post-admixture. In two of these simulations, the observed $r(x_i, x_j) \in \{0.0399, 0.0444\}$ never overlapped the permuted distribution (empirical $p < 0.001$). In contrast, $r(x_i, x_j)$ always overlapped the permuted distribution after $t = 11$ generations under the broad-preference model ($\alpha = 10$) (**Figure S10**).

Thus, not all variants of the ancestry-similarity model generate a positive correlation in global ancestry proportion between mates that is observable 20 generations post-admixture while also allowing for a large population of individuals within intermediate global ancestry proportion. Conversely, results for the social group model demonstrate that even relatively weak social barriers can produce a positive correlation in global ancestry proportion between mates on the timescale of tens of generations, even as the association between social group membership and global ancestry proportion diminishes over time **(Figure S11).**

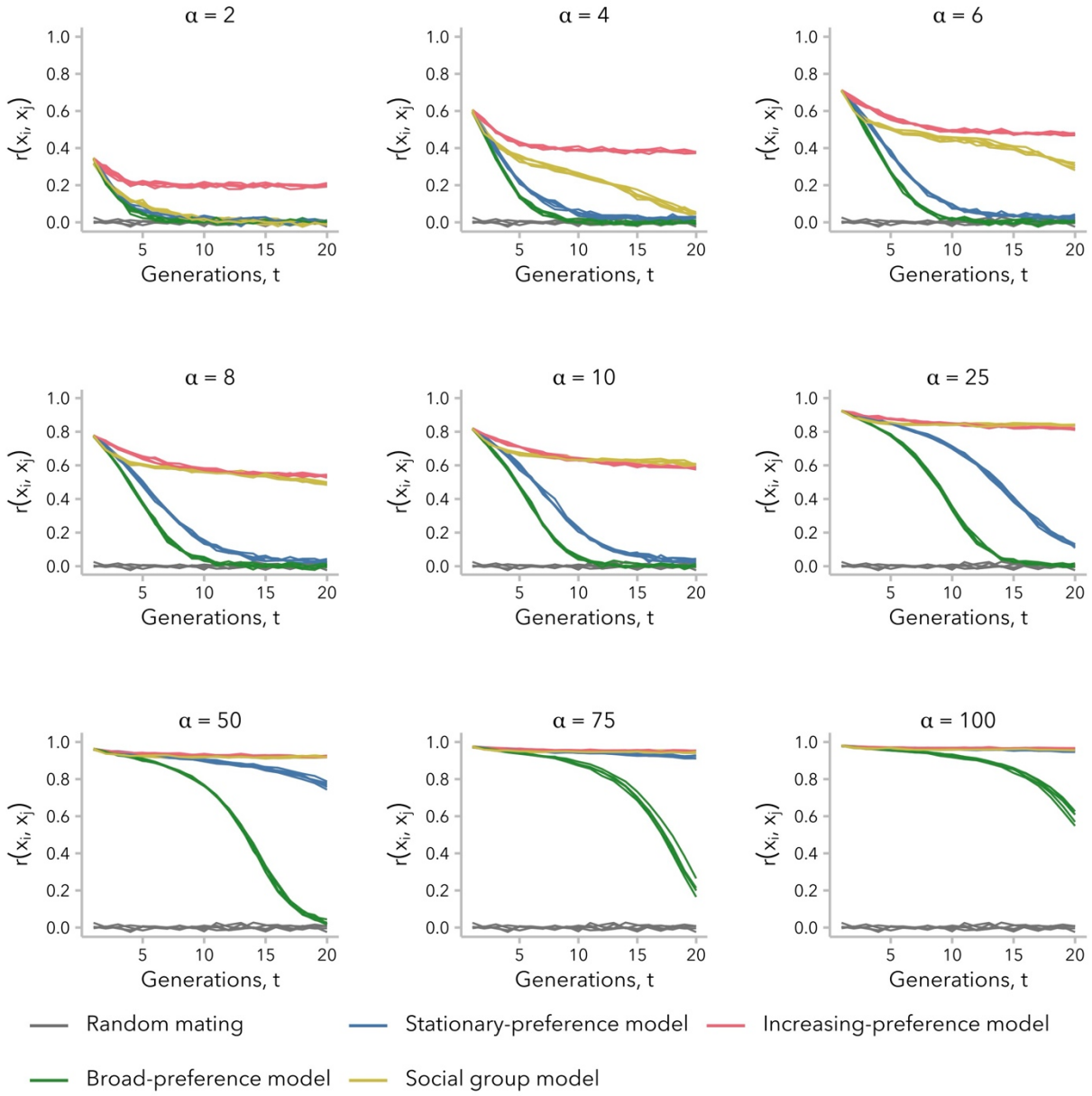

Figure 2. Correlation in global ancestry proportion between mates, $r(x_i, x_j)$, was not constant over time and decayed to near-zero within 20 generations post-admixture in some simulations. Simulations under the stationary-preference (blue; EQUATION 2) and broad-preference (green; EQUATION 4) models did not simultaneously maintain $r(x_i, x_j) \gg 0$ while also allowing for a large population with intermediate global ancestry proportion values, whereas those under the increasing-preference (pink; EQUATION 3) and social group (yellow; EQUATION 5) models did for some α. By definition, $r(x_i, x_j)$ in the first generation after admixture is equal across all simulations performed with the same value of α, regardless of mate-choice model. For the sake of comparison, the same replicate random-mating simulations ($\alpha = 1$; gray) are reproduced in each subplot. See **Figure S6**.

Relationship between correlation in global ancestry proportion between mates and variance in global ancestry proportion across individuals differs between models

To understand why the stationary-preference and broad-preference models did not produce a sustained correlation in global ancestry proportion between mates, $r(x_i, x_j) \gg 0$, over time while the increasing-preference and social group models sometimes did (**Figure 2**), we next considered the variance in global ancestry proportion across individuals in generation t, $\sigma_x^2(t)$. Intuitively, non-random mating requires that individuals in the population vary for the trait that serves as the basis for mate choice: if all potential mates are identical for the relevant phenotype, mating pairs will form randomly regardless of the strength of mate-choice bias. Thus, we hypothesized that our simulations of biased mating would become indistinguishable from random mating when $\sigma_x^2(t)$ became sufficiently small.

Consistent with prior analytic models, $\sigma_x^2(t)$ was initially greater under non-random relative to random mating, regardless of mate-choice model (WRIGHT 1921; VERDU AND ROSENBERG 2011; ZAITLEN *et al.* 2017; GOLDBERG *et al.* 2020; LIANG *et al.* 2024), and decayed more slowly for larger α (**Figure S12**). However, for simulations under the stationary-preference and broad-preference models, $\sigma_x^2(t)$ approached zero within approximately $t = 15$ generations post-admixture under our set of parameters. This timing corresponds to when $r(x_i, x_j) \approx 0$ under these two models, as observed in **Figure 2**. In contrast, under the increasing-preference and social group models, which maintained a positive $r(x_i, x_j)$ at $t = 20$ generations, $\sigma_x^2(t)$ was greater than for random mating for any generation t (all α for the increasing-preference model; $\alpha > 2$ for the social group model).

As predicted, higher $\sigma_x^2(t)$ corresponded to higher $r(x_i, x_j)$ for all four models, at least for early generations post-admixture (**Figure S13**). However, this relationship was not linear and differed across both models and ranges of $\sigma_x^2(t)$. In early generations, when $\sigma_x^2(t)$ is large, $r(x_i, x_j)$ scales approximately linearly with $\sigma_x^2(t)$ under all models (**Figure 3a**). As the admixture process continues, however, we observed that for intermediate values of $\sigma_x^2(t)$, the same $\sigma_x^2(t)$ corresponded to a lower $r(x_i, x_j)$ under the stationary-preference and broad-preference models relative to the other two models (**Figure 3b, c**). In other words, simulations under these two models required greater variance in global ancestry proportion across individuals in order to observe the same correlation in global ancestry proportion between mates. By $t = 20$ generations post-admixture, $\sigma_x^2(t)$ is small and we observed that the same $\sigma_x^2(t)$ corresponded to a higher $r(x_i, x_j)$ under the increasing-preference model than under the social group model (**Figure 3d**). This emphasizes a key distinction between these two models: the social group model sustains a positive $r(x_i, x_j)$ over tens of generations by maintaining higher$\sigma_x^2(t)$, whereas the increasing-preference model instead compensates for very low $\sigma_x^2(t)$ by scaling the mate-choice parameter c by $\sigma_x^2(t)$, increasing the strength of preference in each generation.

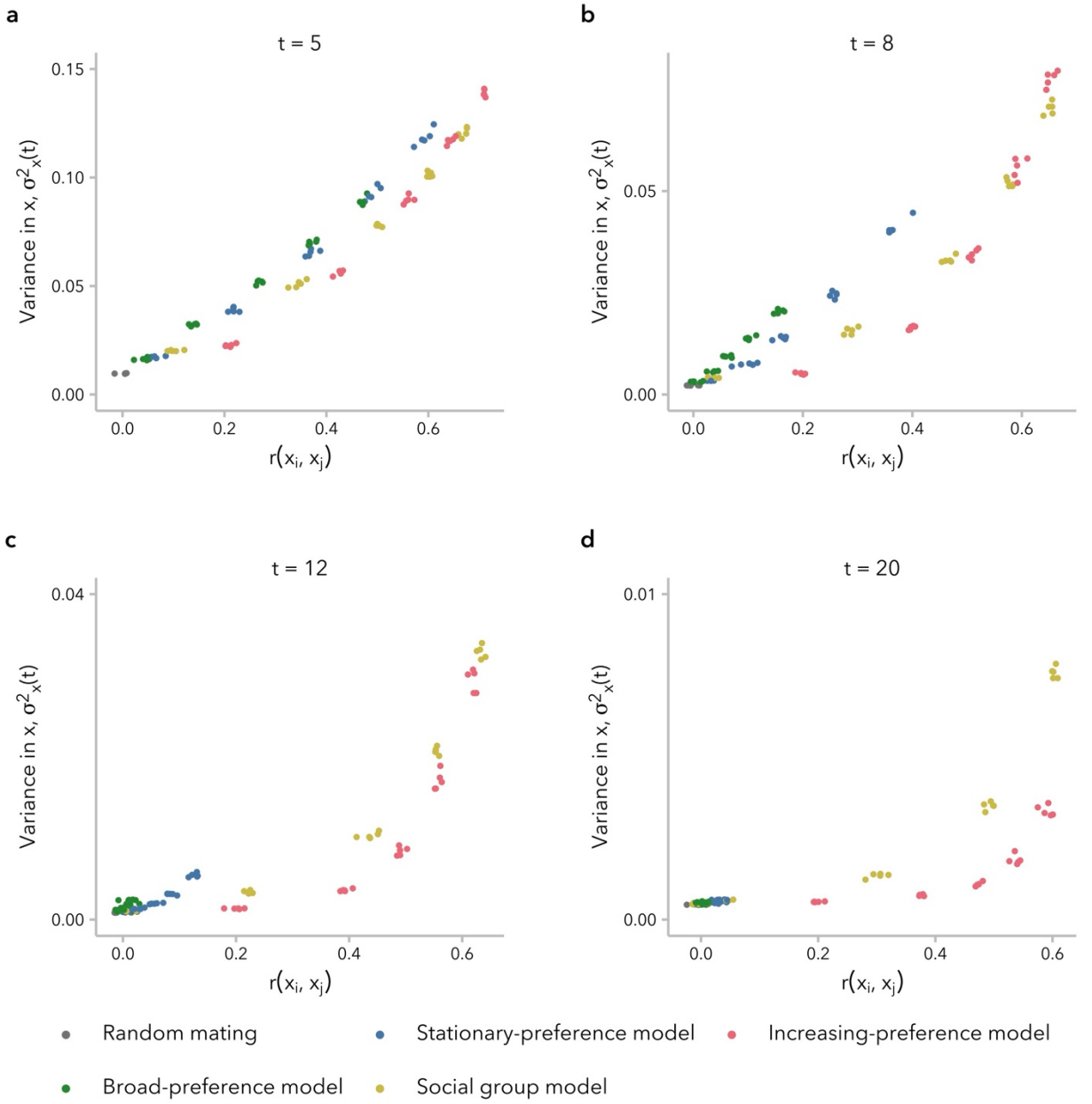

Figure 3. The relationship between variance in global ancestry proportion across individuals, $\sigma_x^2(t)$, and correlation in global ancestry between mates, $r(x_i, x_j)$, differs between models and changes as $\sigma_x^2(t)$ approaches zero. **(a)** In early generations, when $\sigma_x^2(t)$ is larger, there is a quasi-linear relationship between $r(x_i, x_j)$ and $\sigma_x^2(t)$. **(b, c)** As the value of $\sigma_x^2(t)$ decreases, differences between the two models that sustain high $r(x_i, x_j)$ and the two model that do not. **(d)** At generation $t = 20$, a given value of $r(x_i, x_j)$ corresponds to a lower $\sigma_x^2(t)$ under the increasing-preference model relative to the social group model. In other words, the increasing-preference model maintains a high $r(x_i, x_j)$ at $t = 20$ generations post-admixture despite low differentiability of potential mates. Each dot represents one simulation (5 replicates each for $\alpha \in \{1, 2, 4, 6, 8, 10\}$).

Given our broader objective of understanding mechanisms that could potentially explain the correlation in global ancestry proportion between spouses that has been reported in empirical data, in the following sections we focus on the two models that produce $r(x_i, x_j) \gg 0$ for tens of

generations post-admixture: the increasing-preference model and the social group model. Specifically, we compare pairs of simulations performed under these models that produced the same value of $r(x_i, x_j)$ at $t = 20$ generations post-admixture, noting that we did not observe evidence for any effect of global ancestry proportion on reproductive success in these simulations (**Figure S14; Figure S15**).

The same correlation in global ancestry proportion between mates can be explained by multiple patterns of non-random mating

Though commonly used for empirical genetic studies, the correlation in global ancestry proportion between mates is not particularly informative about the underlying distribution of global ancestry proportion, x, within the population. As a general principle, the admixture process ultimately results in a shift in the distribution of x over time from bimodal to unimodal, as two discrete source populations with $x \in \{0,1\}$ converge to a continuous distribution of intermediate x values. This shift to a unimodal distribution occurs within a single generation under random mating; under ancestry-biased mating, we expect the shift to be delayed, as individuals with more extreme x preferentially mate with one another.

We observed that the timing of this shift is delayed even more under the social group model than under the increasing-preference model, whether comparing pairs of simulations matched for mating bias strength, α (**Figure S16**) or for correlation in the global ancestry proportion, $r(x_i, x_j)$. Specifically, we considered the distributions of x at $t = 20$ generations post-admixture, approximating the timing of the onset of admixture for many human populations with African and European ancestry (Zaitlen *et al.* 2017; Hamid *et al.* 2021; Korunes *et al.* 2022; Mas Sandoval *et al.* 2023; Mooney *et al.* 2023). At $t = 20$, we found a unimodal distribution of ancestry proportion for simulations under the increasing-preference model for all α, whereas the social group model produced a bimodal distribution for simulations with $\alpha \geq 7$. For simulations under the social group model with $\alpha < 7$, ancestry proportion was unimodal but with higher variance than simulations under the increasing-preference model with the same correlation between mates **(Figure S17)**.

Differences in the distribution of global ancestry proportion, x, within the population between the increasing-preference and social group models are also reflected in the distribution of mating pairs, (x_i, x_j) at $t = 20$ generations post-admixture. Under the increasing-preference model, the mating pairs form a single cluster with highest density around $(0.5, 0.5)$, reflecting the original equal contributions from the two source populations (**Figure 4a**). In contrast, for a simulation under the social group model with the same correlation in global ancestry proportion between mates, $r(x_i, x_j)$, there were two distinct clusters of mating pairs, reflecting preferential mating within each of two subpopulations (**Figure 4b**). These clusters were identifiable by eye when $r(x_i, x_j) \geq 0.4$ (**Figure S18**). Thus, although the same correlation in global ancestry proportion between mates can be produced by both the increasing-preference and social group models, the underlying structure of non-random mating is not equivalent, and may be distinguishable when $r(x_i, x_j)$ is large.

Given that evidence for ancestry-assortative mating is often assessed in substantially smaller empirical datasets, we also examined whether these differences in mating structure could be observed in a subsample ($n = 100$ individuals) of our simulated population. The correlation in global ancestry proportion between mates is typically visualized as a dot-plot (*e.g.*, (Zou *et al.* 2015;

KORUNES *et al.* 2022)); we found that the two models looked similar when taking this approach (**Figure S19**). However, even with only 100 individuals, hexagonal bin plots (CARR *et al.* 1987) suggested the presence of two discrete clusters of mating pairs in simulations under the social group model with high α (and thus high $r(x_i, x_j)$) (**Figure 4c-d; Figure S20**).

These results, along with similar results using the distribution of the absolute difference in global ancestry proportion between mate pairs, $\Delta_x = |x_i - x_j|$, rather than summarizing it as a correlation coefficient (**Figure S21**), underscore that multiple mating structures can produce very similar correlation in global ancestry proportion between mates and highlight the utility of alternative visualizations for understanding the mating structure in a population of interest.

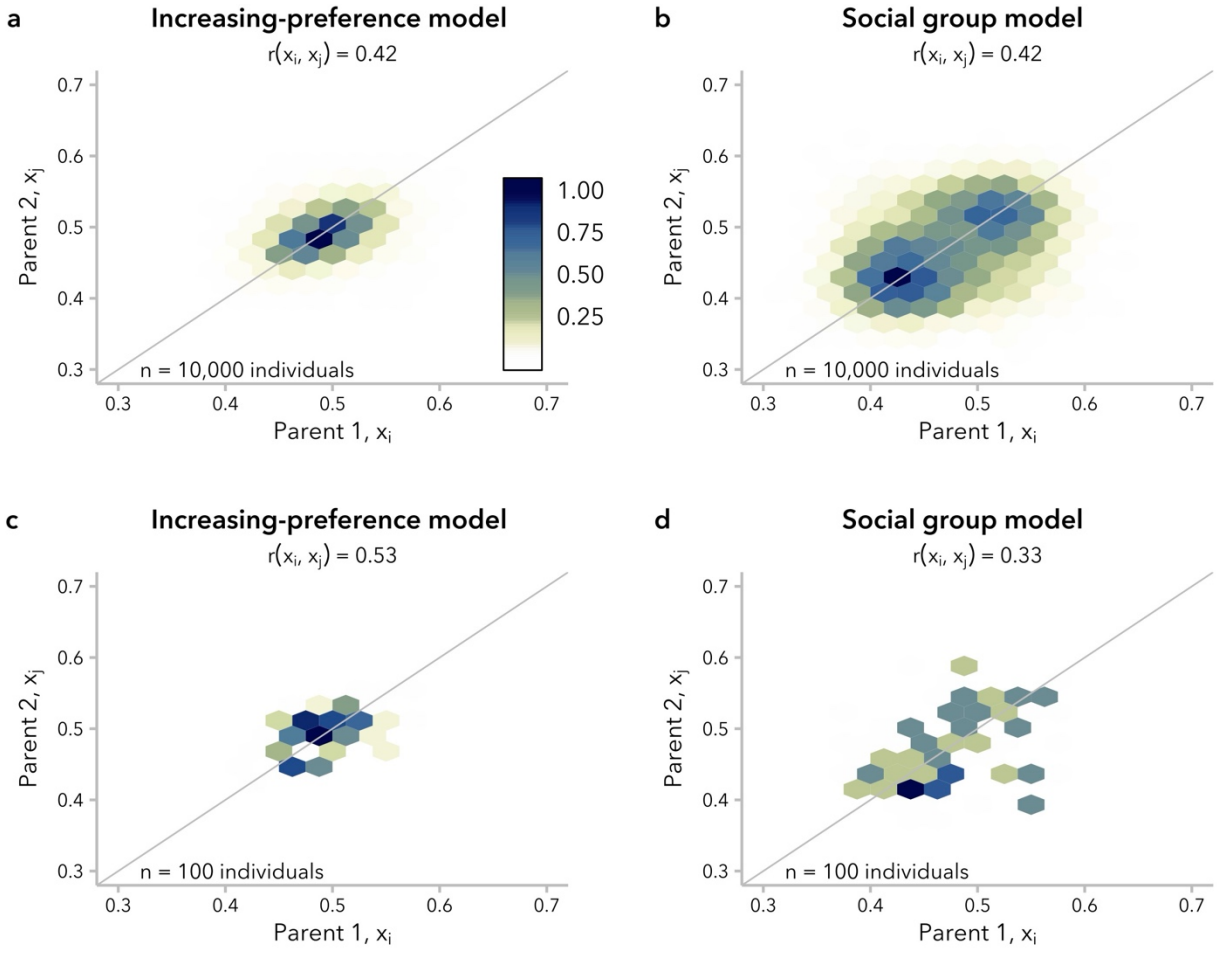

Figure 4. Simulations under the increasing-preference ($\alpha = 5$) and social group ($\alpha = 7$) models produced the same correlation in global ancestry proportion between mates, $r(x_i, x_j)$, at $t = 20$ generations post-admixture but with different underlying mating structure. Hexagonal bin plots represent the correlation in global ancestry proportion between the two parents of individuals in generation $t = 20$. Each hexagon corresponds to a bin of 0.025 global ancestry proportion units, with color encoding the scaled density ($\max = 1$) of mating pairs in each bin. **(a)** Under the increasing-preference model, mating pairs cluster around a single bin of maximum density. **(b)** In contrast, under the social group model, mating pairs form two clusters, representing preferential mating within each of two social groups. All 10,000 individuals are shown. A $y = x$ line is shown for reference. **(c, d)** The same

trends are observed when considering a subsample of $n = 100$ individuals. See **Figure S18, Figure S19,** and **Figure S20**.

Non-random mating produced an excess of long local-ancestry tracts relative to random mating, leading to underestimates for the timing of admixture

Thus far, we have focused on the relationship between mate-choice model and the distribution of global ancestry proportion. We next considered the impact of model choice on the length distribution of local-ancestry tracts, which is used directly or indirectly (*e.g.*, using admixture linkage disequilibrium as a proxy) to infer demographic parameters, including the time since the onset of admixture (MOORJANI *et al.* 2011; GRAVEL 2012; LOH *et al.* 2013; HELLENTHAL *et al.* 2014). Prior work has shown that non-random mating disrupts the decay in local-ancestry tract length due to recombination, resulting in long local-ancestry tracts consistent with more recent admixture than truly occurred (ZAITLEN *et al.* 2017; KORUNES *et al.* 2022). Thus, some methods to correct for the systematic underestimation of the time since admixture due to assortative mating attempt to recapitulate local-ancestry tract length dynamics by matching the empirical correlation between spouses (ZAITLEN *et al.* 2017).

We first compared the median local-ancestry tract length at $t = 20$ generations post-admixture in simulations under the increasing-preference and social group models, matched for correlation in global ancestry proportion between mates, $r(x_i, x_j)$. Differences in median local-ancestry tract length were modest when comparing across α values within a single model, between these two mate-choice models, and between both models and random mating (**Figure 5a**). However, we did observe across all four mate-choice models that larger values of α were associated with longer median local-ancestry tract lengths at generation $t = 20$ (**Figure S22**). Furthermore, under the increasing-preference and social group models — the two models under which $r(x_i, x_j) \gg 0$ at generation $t = 20$ — greater $r(x_i, x_j)$ was also associated with longer median local-ancestry tract length. Additionally, for a given value of $r(x_i, x_j)$, median local-ancestry tract length tended to be longest under the social group model (**Figure 5b**).

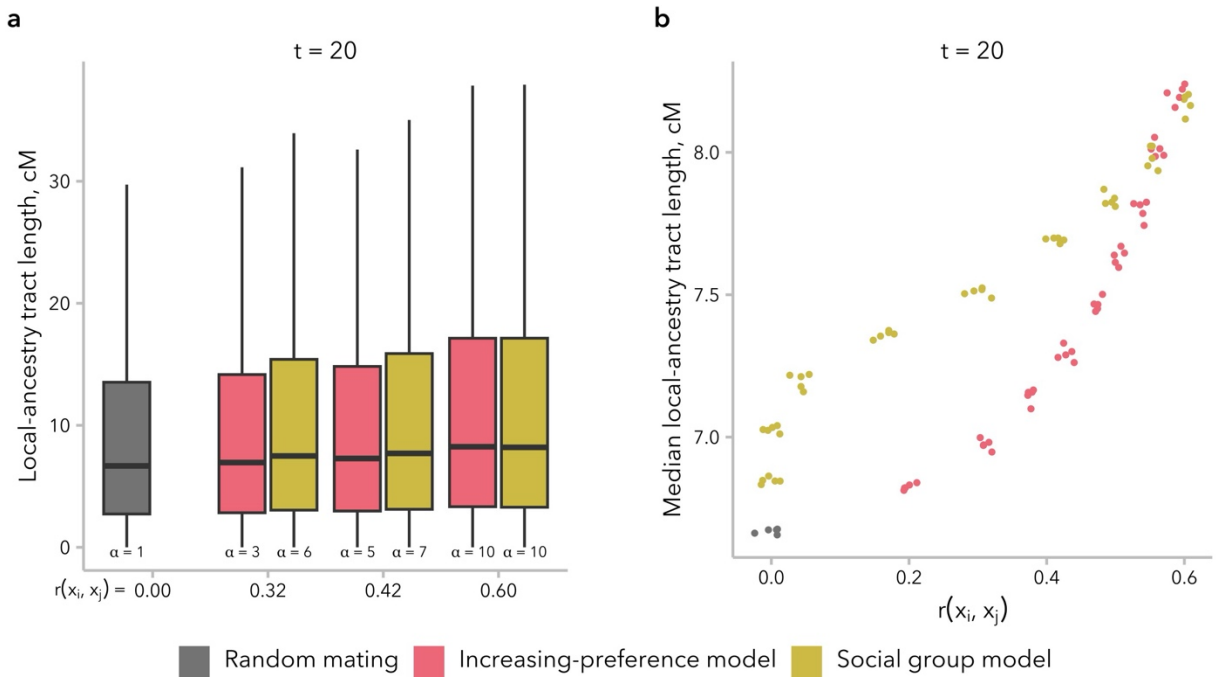

Figure 5. Local-ancestry tract length distributions were similar for simulations under the increasing-preference and social group models, when comparing simulations with similar correlation in global ancestry proportion between mates, $r(x_i, x_j)$. **(a)** The distribution of local-ancestry tract lengths at $t = 20$ generations post-admixture is shown for three representative pairs of simulations, matched for $r(x_i, x_j)$. A random mating control simulation is shown in gray. Because the local-ancestry tract length distribution has a very long tail, the y-axis is truncated at the top whisker (75th percentile + 1.5 × the inter-quartile range). **(b)** Median local-ancestry tract length was similar across models and values of α. However, for the same $r(x_i, x_j)$, median local-ancestry tract length tended to be longer for simulations under the social group model relative to those under the increasing-preference model. Each dot represents one simulation (5 replicates each for $\alpha \in \{1, 2, 4, 6, 8, 10\}$).

To directly test the effects of the increasing-preference and social group models on downstream inference of admixture timing, we fit an exponential to the local-ancestry tract length distribution, with decay rate $\lambda = (t + 1) \times m$, where t represents generations post-admixture and m represents the proportion of individuals from source population 1 contributing to the founding of the admixed populations. From the fit, we then inferred that a single-pulse admixture event occurred t generations before the time of sampling (EQUATION 1 from (GRAVEL 2012)). We observed that the simulated distribution of local-ancestry tracts had an excess of long local-ancestry tracts at $t = 20$ generations post-admixture relative the exponential fit, particularly for simulations with greater $r(x_i, x_j)$ (**Figure 6a, b**). Although slight, this mismatch in distribution shape may prove useful as an indication in empirical data that the effects of non-random mating should be taken into consideration, although it may also be confused for evidence of continuous migration.

As expected based on prior empirical work (ZAITLEN *et al.* 2017; KORUNES *et al.* 2022), we underestimated the true time since admixture, and the discrepancy between the truth and our inferred time increased as $r(x_i, x_j)$ increased (**Figure 6c**). Intriguingly, we found that this discrepancy was established in the first few generations and then grew relatively slowly over time, suggesting that there might be a plateauing of the effect on longer timescales (**Figure S23**). For instance, time since admixture was underestimated by an average of 2.25 generations for $t = 20$

and 4.01 generations for $t = 50$ generations post-admixture. As a result, we observe a bias of similar magnitude under all four model at $t = 20$ generations post-admixture, although $r(x_i, x_j) \approx 0$ under the stationary-preference and broad-preference models (**Figure S24**).

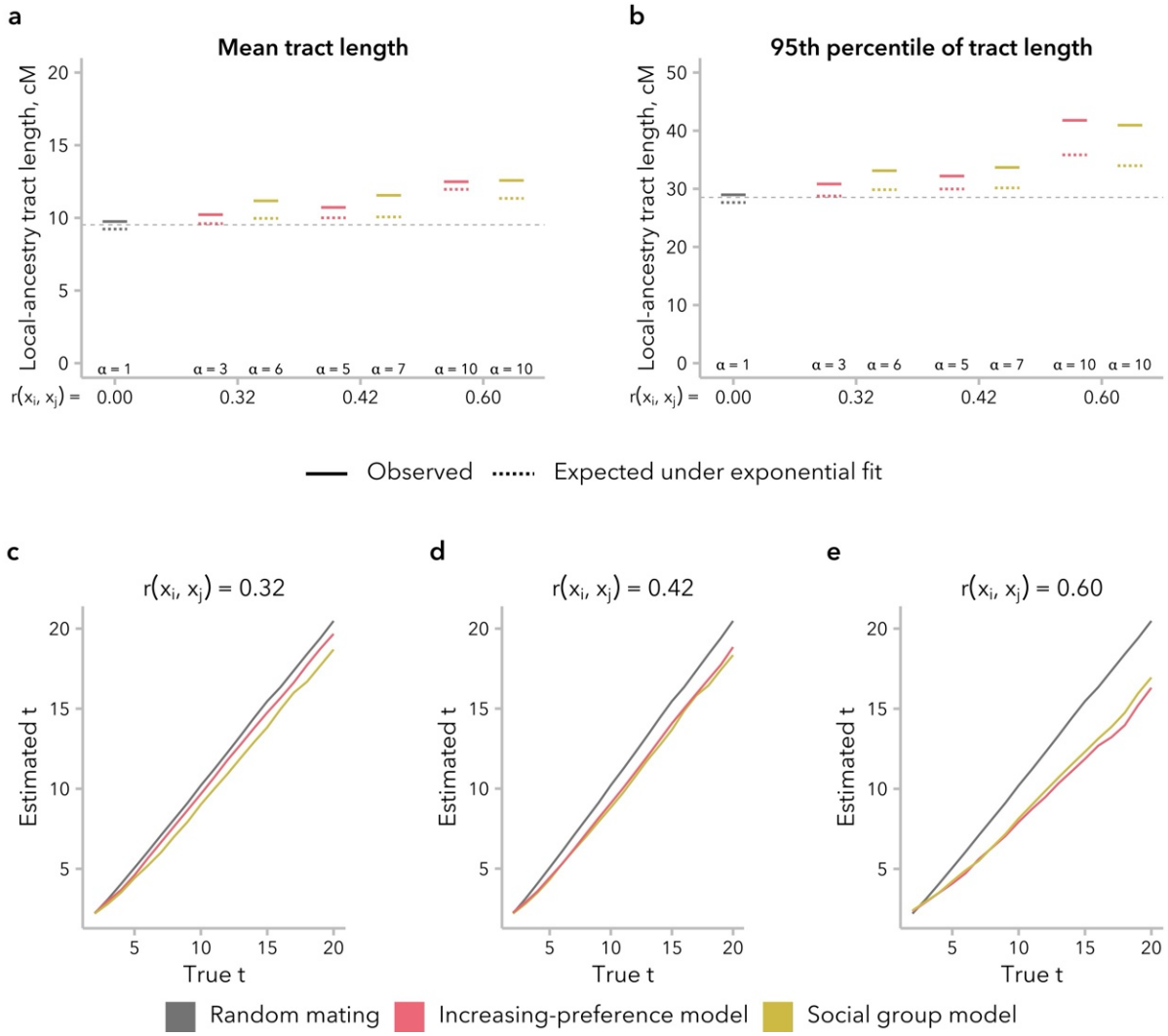

Figure 6. Non-random mating led to underestimation of the time since admixture. For each simulation, an exponential model was fit to the local-ancestry tract length distribution, with decay rate λ. **(a)** For the mean local-ancestry tract length, observed values (solid lines) were similar to those expected under the exponential fit ($1/\lambda$, dotted lines), indicating a good fit to the data. The dashed line at $y = 9.52$ indicates the expected mean local-ancestry tract length for the true values of $t = 20$ and $m = 0.5$. **(b)** However, for the 95th percentile of local-ancestry tract length, observed values (solid lines) were larger than those expected under the exponential fit ($-\ln(1 - 0.95)/\lambda$, dotted lines), particularly when $r(x_i, x_j)$ is high. The dashed line at $y = 28.53$ indicates the expected 95th percentile of local-ancestry tract length for the true values of $t = 20$ and $m = 0.5$. **(c-e)** Estimated time since admixture was similar between the increasing-preference and social group models. As expected, inference was accurate under random mating (gray) and underestimated under both models of non-random mating, with increasing discrepancy between true and inferred values for larger $r(x_i, x_j)$.

The effects of continuous migration on the correlation in global ancestry proportion between mates differed between models and values of α

Realistic models of human admixture likely include more complex dynamics than a single pulse of admixture followed by complete isolation from the source populations, as we have modeled above. To begin to explore the behavior of the increasing-preference and social group models under more complex demographic scenarios, we examined the trajectory of the correlation in global ancestry proportion between mates, $r(x_i, x_j)$, over time in a scenario with continuous migration, wherein 1% of the population in each generation was replaced with migrants from the two source populations. Relative to the single-pulse admixture scenario, we might expect $r(x_i, x_j)$ to be smaller in the continuous-migration scenario for the same generation t and mating bias strength α because new migrants have fewer potential mates with similar global ancestry proportion to choose from compared to individuals born in the admixed population. Furthermore, variance in global ancestry proportion across individuals in the admixed population, $\sigma_x^2(t)$, decreases in each successive generation (**Figure S12**), meaning that new migrants have increasingly dissimilar global ancestry proportion to the average potential mate. On the other hand, mating events between two migrants from the same source population will increase $r(x_i, x_j)$.

We found that the balance between these countervailing effects on $r(x_i, x_j)$ differed between models. Under the increasing-preference model, $r(x_i, x_j)$ initially decreased over time, similar to the scenario with single-pulse admixture. However, for simulations with $\alpha \geq 4$, there was a subsequent increase over time, resulting in a greater $r(x_i, x_j)$ at $t = 20$ generations post-admixture in the scenario with migration than the one without migration (**Figure 7a**). As noted above, the increasing-preference model compensates for the decrease in $\sigma_x^2(t)$ by increasing mate selectiveness over time (**Figure S12**). Consistent with this explanation for the difference between the single-pulse admixture and continuous migration simulations, we observed that the proportion of mating events between migrants increased over time in these simulations (**Figure 7c**). Additionally, under the other two ancestry-similarity models, which do not compensate for the decreased $\sigma_x^2(t)$ over time, we observed that the prevalence of mating events between migrants was constant and that the value of $r(x_i, x_j)$ was similar with or without migration for a given generation t and α (**Figure S25; Figure S26; Figure S27**).

In contrast, the social group model neither takes into consideration similarity in global ancestry proportion, nor increases the strength of mating bias over time. Thus, for simulations under this model, new migrants are equally likely to mate with anyone within their social group regardless of global ancestry proportion; as expected, we observed a constant prevalence in mating events between migrants (**Figure 7d**). Additionally, because $\sigma_x^2(t)$ decreases over time, migrants become increasingly dissimilar from potential mates. As a result, continuous migration always decreased $r(x_i, x_j)$ under this model relative to the single-pulse admixture scenario, controlling for generation and α (**Figure 7c**).

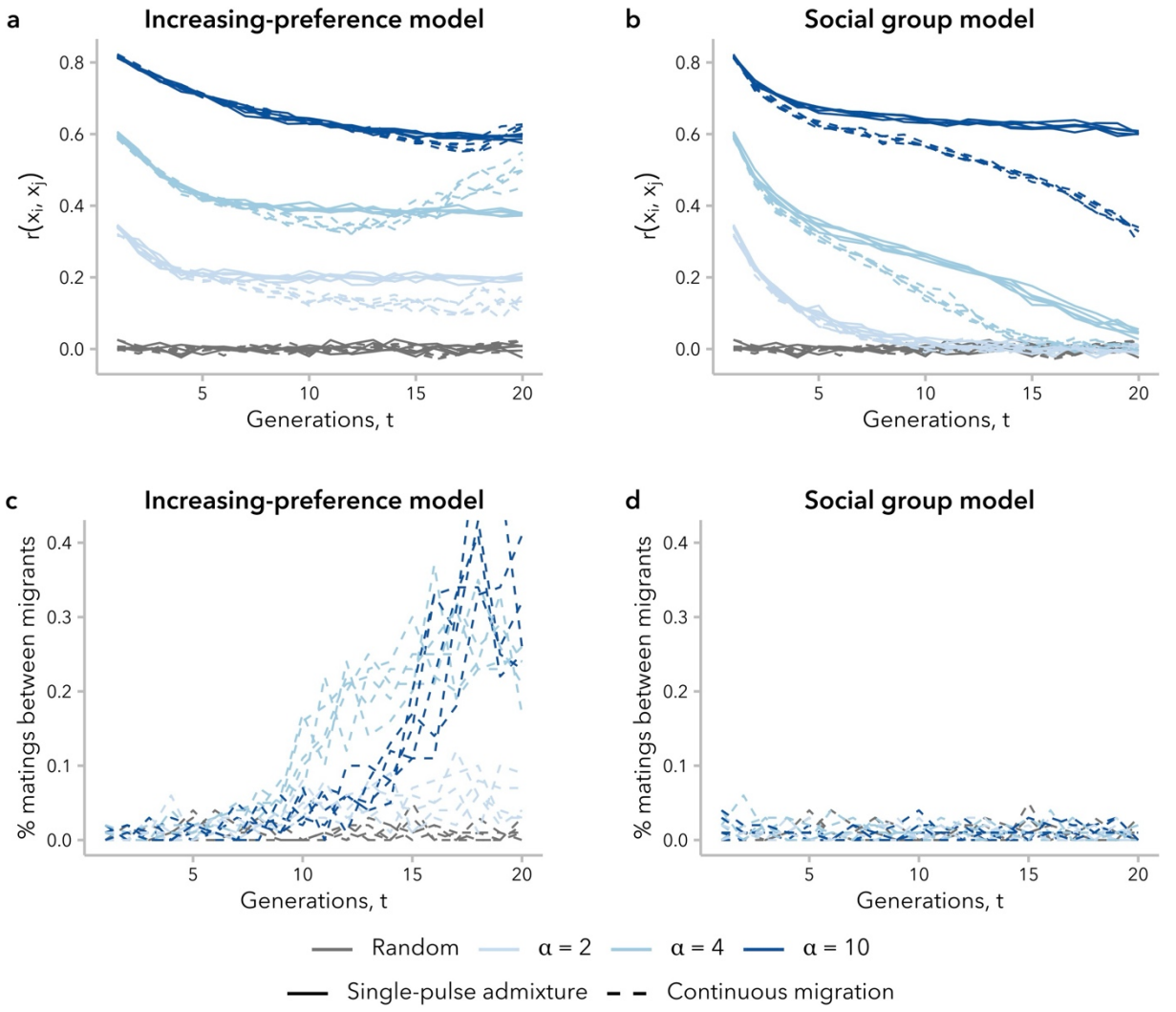

Figure 7. The effects of continuous migration differed between mate-choice models, driven by the percent of mating events between new migrants. **(a, b)** Correlation in global ancestry proportion between mates, $r(x_i, x_j)$ increased over time in simulations under the increasing-preference model with continuous migration, for some α. This behavior was not observed in any simulations without migration (see **Figure 2**) or under the social group model with continuous migration. **(c)** Under the increasing-preference model with continuous migration, mating between migrants was increasingly prevalent over time, and far more frequent than expected under random mating. **(d)** Mating between migrants under the social group model with continuous migration did not occur more often than expected by chance.

Discussion

While it is appreciated that humans, like individuals in many other natural populations, do not choose mates at random, population-genetic theory and methods to account for assortative mating in empirical data remain largely underdeveloped. In the context of ancestry-assortative mating, extension of existing theory on how assortative mating shapes the expected distribution of a trait in a population (WRIGHT 1921; NORRIS *et al.* 2019; KIM *et al.* 2021; BORDER *et al.* 2022; MURALIDHAR *et al.* 2022; HORWITZ *et al.* 2023) is made difficult by ambiguity about what the relevant phenotype is. Furthermore, global ancestry proportion is an unusual quantitative phenotype, in that its trait value is integrated across every locus in the genome. How this genome-wide involvement might impact analyses, such as selection scans and association studies, that attempt to distinguish implicated loci from neutral loci remains unclear. Simulations of ancestry-assortative mating that accurately recapitulate key summaries of empirical data are crucial to unraveling these impacts. Here, we considered two related prerequisite questions: first, are there multiple mechanisms of mate choice compatible with the observed correlation in global ancestry proportion between spouses in human populations? Second, does the choice of a particular mathematical function for defining biased mating meaningfully impact the conclusions drawn from the resulting simulations? We compared four models, including one that considers social groups rather than quantitative similarity in global ancestry proportion as the mechanism of mate choice, to better understand how we ought to think about modeling and correcting for ancestry-assortative mating going forward.

We turn first to assumptions commonly made by statistical genetics methods (ZAITLEN *et al.* 2017; PFENNIG AND LACHANCE 2023; HUANG *et al.* 2024), which focus on the observed empirical correlation in global ancestry between mates: namely, that this correlation is constant over time and that parameters of interest are comparable between empirical data and simulated data with the same correlation coefficient. In our simulations, we find that $r(x_i, x_j)$ is not stable over time and decays toward zero under most models (**Figure 2**). Thus, assuming that bias in mating is constant over time, the correlation in global ancestry proportion between spouses observed in a contemporary sample is likely smaller than it was in previous generations. In addition, we find that multiple models can produce the same $r(x_i, x_j)$ while differing in the underlying mating structure (**Figure 4**) and the distribution of local-ancestry tract lengths (**Figure 5**). However, we find that the effects of these differences between models on estimated time since admixture are likely to be small, likely because the effects on mean local-ancestry tract length are similar (**Figure 6**).

Prior studies that have modeled biased mate choice to develop theory about assortative mating have either not considered how the decrease in variance in global ancestry proportion across individuals over time impacts the correlation in global ancestry proportion between mates (KIM *et al.* 2021; MURALIDHAR *et al.* 2022) or have explicitly modeled a constant correlation coefficient in the face of decreasing variance (HUANG *et al.* 2024). Our work highlights that variance in global ancestry proportion across individuals plays an essential role in determining whether a positive correlation can be observed and, furthermore, whether mating is effectively random (**Figure 3; Figure S12**). Prior theory has also prioritized the role of individual mate-choice preference for similarity in global ancestry proportion ($|x_i - x_j|$). In humans particularly, there is a wide array of social science research to support the role of sociological factors in mating outcomes. To wit, we found that a simplistic model imposing a barrier to mating between two social groups was sufficient to generate signatures of ancestry-assortative mating that could be observed for 20-50 generations post-

admixture. To our knowledge, this type of model has not been used before to model ancestry-assortative mating in admixed populations but may be representative of how social categories like race, ethnicity, and socioeconomic status influence spouse choice.

The four models that we consider in the present study are not the only possible models, but rather represent two classes of model worthy of further theoretical exploration: ancestry-similarity and social group models. For ancestry-similarity models, we have demonstrated that not all variants of this model type can sustain sufficiently high levels of variance in global ancestry proportion across individuals to continue to observe a positive correlation in global ancestry proportion between mates (at least, without additional in-migration events). The increasing-preference model presents a mathematically simple strategy to compensate for this decay in $\sigma_x^2(t)$: increasing the choosiness of individuals. While this is effective in maintaining a high $r(x_i, x_j)$, it is likely unrealistic in practice, making individuals too attuned to small differences between mates (**Figure S2b**). This overcompensation is heightened in the continuous-migration scenario, leading to unexpected (and undesirable) behavior (**Figure 7**). Future development of ancestry-similarity models should consider alternative approaches to tune the selectiveness of individuals over time. For instance, we might want to model a constant degree of bias (*i.e.*, $\frac{\max(\psi_{i,j})}{\min(\psi_{i,j})}$) over time.

In including the social group model in this study, we aimed only to demonstrate that categorical social barriers can mediate ancestry-assortative mating, even when individuals do not directly use ancestry information to make mating decisions. To that end, we designed a proof-of-concept version of this model class, which is likely overly simplistic for drawing conclusions about real-world human populations. Future development of this class could include greater social complexity; for instance, more than two social groups, alternative rules for how individuals "inherit" their social group membership, and asymmetric barriers between groups. Each of these added layers could be implemented in different ways. For example, in a simulation with three groups, barriers might be more permeable between some pairs of groups than others.

A growing body of research suggests that patterns of assortative mating are not stable over time (*e.g.*, (MARE 1991; SUNDE *et al.* 2024)). Under an ancestry-similarity model, this could reflect changes in preference over time, potentially to account for decreasing differences between potential mates (as discussed above). Under a social group model, this could reflect changes in social mobility or acceptance of inter-group mating. Thus, modeling this type of change over time would be an interesting future direction for both classes of model, although it remains outside the scope of the present work.

Here, we focus exclusively on biased mate choice as a mechanism for generating a positive correlation in global ancestry proportion between mates, comparing potential models for implementing that mechanism. Future work should also consider other mechanisms that require non-Wright-Fisher frameworks to incorporate additional parameters (*e.g.*, birth and death rates, dispersal rates, etc.). For instance, in real-world populations, geographic structure (*i.e.*, isolation-by-distance over continuous space) is also a major driver of non-random mating with respect to ancestry. It remains an open question whether geography alone could produce patterns of assortative mating that resemble empirical observations, as well as how geography might interact

with social barriers to shape the opportunities for individuals to encounter one another and act on biased mate preferences.

Taken together, our results emphasize that theory incorporating non-random mating must carefully consider how mate-choice is conceptualized and modeled. While our focus is primarily on how to better model ancestry-assortative mating, we also make a few recommendations for future empirical studies of ancestry-assortative mating in humans. First, observing a correlation in global ancestry proportion between spouses can reflect multiple mechanisms of mate choice and should not be interpreted as unequivocal evidence of a preference for mates with similar global ancestry proportion. Second, the magnitude of the correlation coefficient is limited by variance in global ancestry proportion across individuals. Thus, a positive correlation in global ancestry proportion in a real-world population should be interpreted as specific to the time point sampled. Third, there are multiple mating structures that can give rise to the same Pearson correlation coefficient, and visualization of these patterns (*e.g.*, with a hexagonal bin plot or hurricane plot of Δ_x) may help to disambiguate these possibilities.

As with any simulation study, our results are limited by what we have elected to model or not model. We highlight two important caveats. First, we do not model genetic variation within and between source populations. Empirical analyses rely on these data to first infer global and local ancestry, a process that is sensitive to how researchers define discrete source populations from continuous human genetic variation. In bypassing this step, we cannot comment on how estimation error might interact with our results. Second, we have focused on a single pulse of admixture, turning to a continuous-migration scenario only to highlight an unexpected result from the increasing-preference model. More realistic models of human populations almost certainly involve complex migration dynamics, including multiple pulses of migration; differing contributions from source populations; changes in population size; asymmetries in mate preferences and in the ability of individuals to enact their mate choices; monogamous mating; and multi-way admixture. Inclusion of these additional factors into future models is likely to impact the results. However, each additional factor drastically expands the range of possible implementations and space of parameter values. As such, these more complex models are likely to be most useful when targeted to matching the parameters of a population of interest whose history is well understood and less well suited to a general exploration of parameter space.

Data Availability

All scripts used for simulations, analyses, and figures is available on GitHub at: https://github.com/agoldberglab/ancestry-assortative-mating-simulation.

Acknowledgments

We thank Joshua Schraiber (ORCiD: 0000-0002-7912-2195), Michael M. Hoffman (ORCiD: 0000-0002-4517-1562), John Barton (ORCiD: 0000-0003-1467-421X), Shyamalika Gopalan (ORCiD: 0000-0002-2608-8472), and members of the Goldberg lab for helpful discussions.

Funding

This work was supported by the National Institute of General Medical Sciences of the National Institutes of Health (R35 GM133481 to A.G. and R35 GM146926 to Z.A.S.).

References

Arauna, L. R., J. Bergstedt, J. Choin, J. Mendoza-Revilla, C. Harmant *et al.*, 2022 The genomic landscape of contemporary western Remote Oceanians. Curr Biol 32**:** 4565-4575 e4566.

Avadhanam, S., and A. L. Williams, 2022 Simultaneous inference of parental admixture proportions and admixture times from unphased local ancestry calls. Am J Hum Genet 109**:** 1405-1420.

Beleza, S., J. Campos, J. Lopes, Araujo, II, A. Hoppfer Almada *et al.*, 2012 The admixture structure and genetic variation of the archipelago of Cape Verde and its implications for admixture mapping studies. PLoS One 7**:** e51103.

Blossfeld, H.-P., 2009 Educational assortative marriage in comparative perspective. Annual Review of Sociology 35**:** 513-530.

Bonilla, C., M. D. Shriver, E. J. Parra, A. Jones and J. R. Fernandez, 2004 Ancestral proportions and their association with skin pigmentation and bone mineral density in Puerto Rican women from New York city. Hum Genet 115**:** 57-68.

Border, R., G. Athanasiadis, A. Buil, A. J. Schork, N. Cai *et al.*, 2022 Cross-trait assortative mating is widespread and inflates genetic correlation estimates. Science 378**:** 754-761.

Browning, J. R., 1951 Anti-miscegenation laws in the united states. Duke Bar Journal 1**:** 26-41.

Burger, R., and K. A. Schneider, 2006 Intraspecific competitive divergence and convergence under assortative mating. Am Nat 167**:** 190-205.

Burley, N., 1983 The meaning of assortative mating. Ethology and Sociobiology 4**:** 191-203.

Buss, D. M., and M. Barnes, 1986 Preferences in human mate selection. Journal of Personality and Social Psychology 50**:** 559-570.

Carr, D. B., R. J. Littlefield, W. L. Nicholson and J. S. Littlefield, 1987 Scatterplot matrix techniques for large n. Journal of the American Statistical Association 82**:** 424-436.

Chiappori, P.-A., 2020 The theory and empirics of the marriage market. Annual Review of Economics 12**:** 547-578.

De La Mare, J. K., and A. J. Lee, 2023 Assortative preferences for personality and online dating apps: Individuals prefer profiles similar to themselves on agreeableness, openness, and extraversion. Personality and Individual Differences 208**:** 112185.

Dieckmann, U., and M. Doebeli, 1999 On the origin of species by sympatric speciation. Nature 400**:** 354-357.

Domingue, B. W., J. Fletcher, D. Conley and J. D. Boardman, 2014 Genetic and educational assortative mating among US adults. Proc Natl Acad Sci U S A 111**:** 7996-8000.

Fibla, J., I. Maceda, M. Laplana, M. Guerrero, M. M. Alvarez *et al.*, 2022 The power of geohistorical boundaries for modeling the genetic background of human populations: The case of the rural catalan Pyrenees. Front Genet 13**:** 1100440.

Fisher, R. A., 1918 The correlation between relatives on the supposition of Mendelian inheritance. Transactions of the Royal Society of Edinburgh 52**:** 399-433.

Fogel, A. S., E. M. McLean, J. B. Gordon, E. A. Archie, J. Tung *et al.*, 2021 Genetic ancestry predicts male-female affiliation in a natural baboon hybrid zone. Anim Behav 180**:** 249-268.

Funk, E. R., N. A. Mason, S. Palsson, T. Albrecht, J. A. Johnson *et al.*, 2021 A supergene underlies linked variation in color and morphology in a holarctic songbird. Nat Commun 12**:** 6833.

Goldberg, A., A. Rastogi and N. A. Rosenberg, 2020 Assortative mating by population of origin in a mechanistic model of admixture. Theor Popul Biol 134**:** 129-146.

Gravel, S., 2012 Population genetics models of local ancestry. Genetics 191**:** 607-619.

Greenwood, J., N. Guner, G. Kocharkov and C. Santos, 2014 Marry your like: Assortative mating and income inequality. American Economic Review 104**:** 348-353.

Haller, B. C., J. Galloway, J. Kelleher, P. W. Messer and P. L. Ralph, 2019 Tree-sequence recording in SLiM opens new horizons for forward-time simulation of whole genomes. Mol Ecol Resour 19**:** 552-566.

Haller, B. C., and P. W. Messer, 2023 SLiM 4: Multispecies eco-evolutionary modeling. Am Nat 201**:** E127-E139.

Hamid, I., K. L. Korunes, S. Beleza and A. Goldberg, 2021 Rapid adaptation to malaria facilitated by admixture in the human population of cabo verde. eLife 10.

Hellenthal, G., G. B. J. Busby, G. Band, J. F. Wilson, C. Capelli *et al.*, 2014 A genetic atlas of human admixture history. Science 343**:** 747-751.

Henz, U., and C. Mills, 2017 Social class origin and assortative mating in Britain, 1949–2010. Sociology 52**:** 1217-1236.

Horwitz, T. B., J. V. Balbona, K. N. Paulich and M. C. Keller, 2023 Evidence of correlations between human partners based on systematic reviews and meta-analyses of 22 traits and UK biobank analysis of 133 traits. Nat Hum Behav 7**:** 1568-1583.

Howe, L. J., T. Battram, T. T. Morris, F. P. Hartwig, G. Hemani *et al.*, 2021 Assortative mating and within-spouse pair comparisons. PLoS Genet 17**:** e1009883.

Huang, J., N. Kleman, S. Basu, M. D. Shriver and A. A. Zaidi, 2024 Interpreting SNP heritability in admixed populations. bioRxiv.

Jiang, Y., D. I. Bolnick and M. Kirkpatrick, 2013 Assortative mating in animals. Am Nat 181**:** E125-138.

Kalmijn, M., 1998 Intermarriage and homogamy: Causes, patterns, trends. Annu Rev Sociol 24**:** 395-421.

Keddy-Hector, A. C., 1992 Mate choice in non-human primates. American Zoologist 32**:** 62-70.

Kim, J., M. D. Edge, A. Goldberg and N. A. Rosenberg, 2021 Skin deep: The decoupling of genetic admixture levels from phenotypes that differed between source populations. Am J Phys Anthropol 175**:** 406-421.

Kirkpatrick, M., 1982 Sexual selection and the evolution of female choice. Evolution 36**:** 1-12.

Klinkova, E., J. K. Hodges, K. Fuhrmann, T. de Jong and M. Heistermann, 2005 Male dominance rank, female mate choice and male mating and reproductive success in captive chimpanzees. International Journal of Primatology 26**:** 357-484.

Kondrashov, A. S., 1983 Multilocus model of sympatric speciation I. One character. Theoretical Population Biology 24**:** 121-135.

Kopp, M., M. R. Servedio, T. C. Mendelson, R. J. Safran, R. L. Rodriguez *et al.*, 2018 Mechanisms of assortative mating in speciation with gene flow: Connecting theory and empirical research. Am Nat 191**:** 1-20.

Korunes, K. L., G. B. Soares-Souza, K. Bobrek, H. Tang, Araujo, II *et al.*, 2022 Sex-biased admixture and assortative mating shape genetic variation and influence demographic inference in admixed Cabo Verdeans. G3 (Bethesda) 12.

Lande, R., 1981 Models of speciation by sexual selection on polygenic traits. Proc Natl Acad Sci U S A 78**:** 3721-3725.

Liang, M., M. Shishkin, V. Shchur and R. Nielsen, 2024 Understanding admixture fractions: Theory and estimation of gene-flow. J Math Biol 89**:** 47.

Loh, P. R., M. Lipson, N. Patterson, P. Moorjani, J. K. Pickrell *et al.*, 2013 Inferring admixture histories of human populations using linkage disequilibrium. Genetics 193**:** 1233-1254.

Luo, S., and E. C. Klohnen, 2005 Assortative mating and marital quality in newlyweds: A couple-centered approach. J Pers Soc Psychol 88**:** 304-326.

Mare, R. D., 1991 Five decades of educational assortative mating. American Sociological Review 56**:** 15-32.

Mas Sandoval, A., S. Mathieson and M. Fumagalli, 2023 The genomic footprint of social stratification in admixing American populations. eLife 12**:** 2022.2011.2016.516754.

Melo, M. C., C. Salazar, C. D. Jiggins and M. Linares, 2009 Assortative mating preferences among hybrids offers a route to hybrid speciation. Evolution 63**:** 1660-1665.

Mooney, J. A., L. Agranat-Tamir, J. K. Pritchard and N. A. Rosenberg, 2023 On the number of genealogical ancestors tracing to the source groups of an admixed population. Genetics 224.

Moorjani, P., N. Patterson, J. N. Hirschhorn, A. Keinan, L. Hao *et al.*, 2011 The history of african gene flow into southern europeans, levantines, and jews. PLoS Genet 7**:** e1001373.

Muralidhar, P., G. Coop and C. Veller, 2022 Assortative mating enhances postzygotic barriers to gene flow via ancestry bundling. Proc Natl Acad Sci U S A 119**:** e2122179119.

Nagoshi, C. T., R. C. Johnson and G. P. Danko, 1990 Assortative mating for cultural identification as indicated by language use. Behav Genet 20**:** 23-31.

Nagylaki, T., 1978 The correlation between relatives with assortative mating. Ann Hum Genet 42**:** 131-137.

Natola, L., S. S. Seneviratne and D. Irwin, 2022 Population genomics of an emergent tri-species hybrid zone. Mol Ecol 31**:** 5356-5367.

Norris, E. T., L. Rishishwar, L. Wang, A. B. Conley, A. T. Chande *et al.*, 2019 Assortative mating on ancestry-variant traits in admixed latin American populations. Front Genet 10**:** 359.

Otto, S. P., M. R. Servedio and S. L. Nuismer, 2008 Frequency-dependent selection and the evolution of assortative mating. Genetics 179**:** 2091-2112.

Parra, F. C., R. C. Amado, J. R. Lambertucci, J. Rocha, C. M. Antunes *et al.*, 2003 Color and genomic ancestry in Brazilians. Proc Natl Acad Sci U S A 100**:** 177-182.

Pennings, P. S., M. Kopp, G. Meszena, U. Dieckmann and J. Hermisson, 2008 An analytically tractable model for competitive speciation. Am Nat 171**:** E44-71.

Pfennig, A., and J. Lachance, 2023 Challenges of accurately estimating sex-biased admixture from X chromosomal and autosomal ancestry proportions. Am J Hum Genet 110**:** 359-367.

Powell, D. L., B. M. Moran, B. Y. Kim, S. M. Banerjee, S. M. Aguillon *et al.*, 2021 Two new hybrid populations expand the swordtail hybridization model system. Evolution 75**:** 2524-2539.

Rettelbach, A., M. Kopp, U. Dieckmann and J. Hermisson, 2013 Three modes of adaptive speciation in spatially structured populations. Am Nat 182**:** E215-234.

Risch, N., S. Choudhry, M. Via, A. Basu, R. Sebro *et al.*, 2009 Ancestry-related assortative mating in Latino populations. Genome Biol 10**:** R132.

Robinson, C. E., H. Thyagarajan and A. K. Chippindale, 2023 Evolution of reproductive isolation in a long-term evolution experiment with Drosophila melanogaster: 30 years of divergent life-history selection. Evolution 77**:** 1756-1768.

Robinson, M. R., A. Kleinman, M. Graff, A. A. E. Vinkhuyzen, D. Couper *et al.*, 2017 Genetic evidence of assortative mating in humans. Nature Human Behaviour 1**:** 0016.

Schumer, M., D. L. Powell, P. J. Delclos, M. Squire, R. Cui *et al.*, 2017 Assortative mating and persistent reproductive isolation in hybrids. Proc Natl Acad Sci U S A 114**:** 10936-10941.

Schwartz, C. R., 2013 Trends and variation in assortative mating: Causes and consequences. Annual Review of Sociology 39**:** 451-470.

Sebro, R., T. J. Hoffman, C. Lange, J. J. Rogus and N. J. Risch, 2010 Testing for non-random mating: Evidence for ancestry-related assortative mating in the Framingham heart study. Genet Epidemiol 34**:** 674-679.

Sebro, R., G. M. Peloso, J. Dupuis and N. J. Risch, 2017 Structured mating: Patterns and implications. PLoS Genet 13**:** e1006655.

Sebro, R., and N. J. Risch, 2012 A brief note on the resemblance between relatives in the presence of population stratification. Heredity (Edinb) 108**:** 563-568.

Seger, J., 1985 Unifying genetic models for the evolution of female choice. Evolution 39**:** 1185-1193.

Setchell, J. M., and E. J. Wickings, 2006 Mate choice in male mandrills (mandrillus sphinx). Ethology 112: 91-99.

Shriver, M. D., E. J. Parra, S. Dios, C. Bonilla, H. Norton *et al.*, 2003 Skin pigmentation, biogeographical ancestry and admixture mapping. Hum Genet 112: 387-399.

Smadja, C. M., E. Loire, P. Caminade, D. Severac, M. Gautier *et al.*, 2022 Divergence of olfactory receptors associated with the evolution of assortative mating and reproductive isolation in mice. Peer Community Journal 2.

Smieja, M., and M. Stolarski, 2018 Assortative mating for emotional intelligence. Curr Psychol 37: 180-187.

Spear, M. L., A. Diaz-Papkovich, E. Ziv, J. M. Yracheta, S. Gravel *et al.*, 2020 Recent shifts in the genomic ancestry of Mexican Americans may alter the genetic architecture of biomedical traits. eLife 9.

Sunde, H. F., N. H. Eftedal, R. Cheesman, E. C. Corfield, T. H. Kleppesto *et al.*, 2024 Genetic similarity between relatives provides evidence on the presence and history of assortative mating. Nat Commun 15: 2641.

Tenesa, A., K. Rawlik, P. Navarro and O. Canela-Xandri, 2016 Genetic determination of height-mediated mate choice. Genome Biol 16: 269.

Torche, F., 2010 Educational assortative mating and economic inequality: A comparative analysis of three latin American countries. Demography 47: 481-502.

Tung, J., M. J. Charpentier, S. Mukherjee, J. Altmann and S. C. Alberts, 2012 Genetic effects on mating success and partner choice in a social mammal. Am Nat 180: 113-129.

Van Belle, S., A. Estrada, T. E. Ziegler and K. B. Strier, 2009 Sexual behavior across ovarian cycles in wild black howler monkeys (alouatta pigra): Male mate guarding and female mate choice. Am J Primatol 71: 153-164.

Veller, C., and G. M. Coop, 2024 Interpreting population- and family-based genome-wide association studies in the presence of confounding. PLoS Biol 22: e3002511.

Verdu, P., and N. A. Rosenberg, 2011 A general mechanistic model for admixture histories of hybrid populations. Genetics 189: 1413-1426.

Woodman, J. P., E. F. Cole, J. A. Firth, C. M. Perrins and B. C. Sheldon, 2023 Disentangling the causes of age-assortative mating in bird populations with contrasting life-history strategies. J Anim Ecol 92: 979-990.

Wright, S., 1921 Systems of mating. III. Assortative mating based on somatic resemblance. Genetics 6: 144-161.

Wright, S., 1950 Genetical structure of populations. Nature 166: 247-249.

Xie, Y., S. Cheng and X. Zhou, 2015 Assortative mating without assortative preference. Proc Natl Acad Sci U S A 112: 5974-5978.

Yamamoto, K., K. Sonehara, S. Namba, T. Konuma, H. Masuko *et al.*, 2023 Genetic footprints of assortative mating in the Japanese population. Nat Hum Behav 7: 65-73.

Zaitlen, N., S. Huntsman, D. Hu, M. Spear, C. Eng *et al.*, 2017 The effects of migration and assortative mating on admixture linkage disequilibrium. Genetics 205: 375-383.

Zou, J. Y., D. S. Park, E. G. Burchard, D. G. Torgerson, M. Pino-Yanes *et al.*, 2015 Genetic and socioeconomic study of mate choice in Latinos reveals novel assortment patterns. Proc Natl Acad Sci U S A 112: 13621-13626.